IL NUOVO CIMENTO Online First
DOI 10.1393/ncc/i2011-10945-3

COLLOQUIA: Channeling 2010

Polarization properties of DCR from relativistic channeled electrons

K. B. KOROTCHENKO(*) and YU. L. PIVOVAROV
Department of Theoretical and Experimental Physics, Tomsk Polytechnic University
Lenin Ave. 30, 634050 Tomsk, Russia

(ricevuto il 22 Dicembre 2010; pubblicato online il 29 Agosto 2011)

Summary. — Based on the modification of the dynamic theory of DCR from axially channeled electrons, the formulas for the angular distributions of the directions of DCR linear polarization are obtained. The calculations of the angular distributions of the directions of DCR linear polarization from planar ($\gamma = 80$) and axially ($\gamma = 20$) channeled electrons in Si and LiF crystals are performed. These calculations show significant differences in the polarization properties of DCR compared with those of PXR, which can be useful in future experiments on the observation of DCR.

PACS `41.60.-m` – Radiation by moving charges.
PACS `61.05.cp` – X-ray diffraction.

1. – Introduction

The diffracted channeling radiation (DCR) a the specific kind of radiation, the combined effect of channeling radiation and its simultaneous diffraction that is generated by channeled electrons and positrons in crystals at Bragg angles. The parametric X-ray radiation (PXR), the diffraction of relativistic electron eigenfield (virtual photons) in a crystal into real ones, in contrast to DCR, is well studied, both theoretically and experimentally. The first theoretical description of DCR in the frame of the kinematic theory was done in [1, 2], and then in [3], in the frame of dynamical theory, for planar channeled electrons and positrons. Later, the theory was extended to take into account the band structure of transverse energy levels and initial population of levels (states) of planar channeled [4] and axially channeled [5] electrons. The developed theory was used to perform detailed calculations of the intensity of DCR angular distributions for both planar [4, 6, 7] and axial channeling [8, 9]. It should be underlined that both PXR and DCR are characterized by specific polarization properties. As to PXR, the predicted theoretical polarization properties are successfully confirmed by experimental measurements of the linear polarization degree and angular distributions of the directions of DCR linear

(*) E-mail: `korotchenko@tpu.ru`

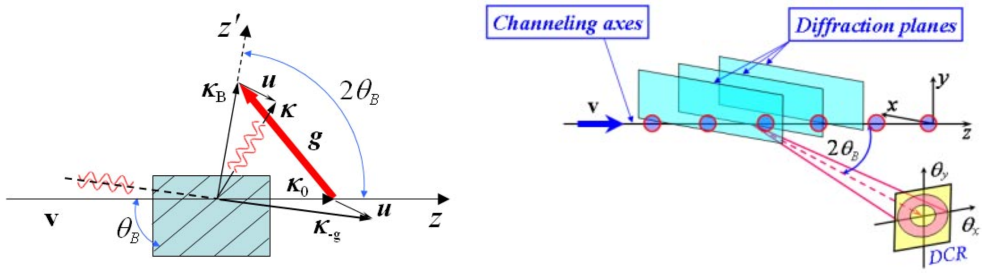

Fig. 1. – Formation of DCR by the axially channeled electrons.

polarization from moderately relativistic electrons, see refs. [10-16]. Here, we show that DCR, compared to PXR, has very specific polarization properties.

2. – DCR matrix elements

To describe the DCR polarization for axial and planar channeling, we use the results of calculations of DCR spectral-angular distributions obtained in [3-9].

Figure 1 shows the geometry of a problem, when the Z-axis is directed along the channeling axis. The electron motion in this direction is described by plane waves: prior to the emission, $\exp[\mathrm{i}p_z z]$, and after the emission, $\exp[\mathrm{i}p'_z z]$. Then, according to [3, 5], the matrix element of the DCR probability can be written as

$$M_{if} = \frac{e}{\gamma m_e c} \langle \phi_f, p'_z | \vec{A}\hat{p} | \phi_i, p_z \rangle . \tag{1}$$

Here, γ is the relativistic factor, $\hat{p} = (\hat{p}_\perp, p_z)$ the electron momentum operator, ϕ_i the wave function of the transverse motion of channeled electrons in state i, $\vec{A}$ is the vector potential of the electromagnetic field, which due to the periodicity of the crystal structure can be presented in Bloch form [3]

$$\vec{A} = \sum_h \vec{A}_h \exp[\mathrm{i}\vec{\kappa}_h \vec{r}] + \mathrm{c.c.} = \sum_h \sum_\tau A_{\tau h} \vec{\varepsilon}_{\tau h} \exp[\mathrm{i}\vec{\kappa}_h \vec{r}] + \mathrm{c.c.} \tag{2}$$

In the two-wave approximation, the vector $\vec{h}$ can take values $(0, \vec{g}\,)$, where $\vec{g}$ is the reciprocal lattice vector for the chosen diffraction plane, $\vec{\kappa}_h$ is the wave vector of a photon, $\vec{\varepsilon}_{\tau h}$ is the polarization vector, $\tau = \perp, \|$ is an index indicating the components of the polarization vector $\vec{\varepsilon}_{\tau h}$, which are normal ($\sigma$-polarization) and tangential (π-polarization) to the plane formed by vectors $\vec{\kappa}$ and $\vec{\kappa}_{-g}$, see fig. 1. Note also that for the linear polarization $A^*_{\tau h} = A_{\tau h}$.

Substitution of eq. (2) into eq. (1) results in the matrix element for the emission of τ-polarized photons

$$\begin{aligned} M_\tau^{if} &= -(e/\gamma mc) \\ &\times (\langle \phi_f, p'_z | A_{\tau 0} \vec{\varepsilon}_{\tau 0} \exp[-\mathrm{i}\vec{\kappa}_0 \vec{r}] \hat{p} | \phi_i, p_z \rangle + \langle \phi_f, p'_z | A_{\tau g} \exp[-\mathrm{i}\vec{\kappa}_g \vec{r}] \vec{\varepsilon}_{\tau g} \hat{p} | \phi_i, p_z \rangle) . \end{aligned} \tag{3}$$

The first term in this sum, according ref. [3], corresponds to a Cherenkov radiation at channeling (if $i = f$ and $v > c/\sqrt{\varepsilon_0}$), or to channeling radiation, CR (if $i \neq f$). The second term at $i \neq f$ describes the DCR, X-rays at the Bragg angles (see fig. 1) and at $i = f$ it describes the PXR, X-rays from the channeled particle.

Let us first consider DCR from axially channeled electrons. Using the dipole approximation and the relation $\langle f|\hat{p}_\perp|i\rangle = -\mathrm{i}\gamma m_e \Omega_{if}\langle f|r_\perp|i\rangle$, one can rewrite the second term in (3) in the form

$$\begin{aligned}(4)\quad & 2c\sqrt{1+W_\tau^2}M^{if}_{-g\tau} = \\ & \mathrm{i}eA_{\tau 0}\left(\langle \phi_f, p'_z|\, c\beta\varepsilon_{\tau g z}\vec{\kappa}_{-g}\left(x\vec{\varepsilon}_{\|0} + y\vec{\varepsilon}_{\perp 0}\right) + \Omega_{if}\vec{\varepsilon}_{\tau g}\left(x\vec{\varepsilon}_{\|0} + y\vec{\varepsilon}_{\perp 0}\right)|\phi_i, p_z\rangle\right).\end{aligned}$$

Here we have denoted: $\vec{r} = (r_\perp, z)$, $\vec{\kappa}_{-g} = \vec{\kappa} - \vec{g} = \vec{\kappa}_0 + \vec{u}$ is the wave vector of the virtual photon (fig. 1); $\varepsilon_{\tau g z}$ is the Z-component of $\vec{\varepsilon}_{\tau g}$, $\beta = v/c$ (v is the electron velocity along the channeling axis); $\hbar\Omega_{if} = (E_i - E_f)$ is the difference between the electron transverse energies in the initial i and final f states. In eq. (4), we rewrite the vector $r_\perp$ in the form $r_\perp = x\vec{\varepsilon}_{\|0} + y\vec{\varepsilon}_{\perp 0}$ using the polarization components $\vec{\varepsilon}_{\|0}$ and $\vec{\varepsilon}_{\perp 0}$ of virtual photons. Writing the formula (4), we have taken into account that in the two-wave approximation [3] the vector potential components of $A_{\tau g}$ can be written in the form

$$(5)\qquad A_{\tau g} = A_{\tau 0}/2\sqrt{1+W_\tau^2},$$

where W_τ is very similar to the so-called “resonance error”, which occurs in the theory of real X-rays diffraction in a crystal in many-waves approximation, see, *e.g.*, [17]. According to [17], this value is the deviation measure from the conditions of Bragg diffraction.

Note that formula (4), describing the DCR matrix element at axial channeling, results in the formula obtained in [3] for DCR at planar channeling, when the X-component of the vector $r_\perp$ is zero, *i.e.* $(r_\perp)_x = x\vec{\varepsilon}_{\|0} = 0$. In this case the wave functions ϕ_i and ϕ_f describe the quantum states of the transverse motion of the electron at planar channeling.

Following [16], we introduce the angular coordinates θ_x and θ_y, describing the DCR photon wave vector deviation from the Bragg direction: $\theta_{x,y} = c(\vec{\kappa} - \vec{\kappa}_B)|_{x,y}\omega_B^{-1} = cu_{x,y}\omega_B^{-1}$ (fig. 1), where $\vec{\kappa}_B = \vec{\kappa}_0 + \vec{g}$ and $\vec{\kappa} = \vec{\kappa}_B + \vec{u}$ is the wave vector of the DCR photon, and $\vec{u} = (\theta_x, \theta_y)\omega_B/c$. In addition, the polarization components $\vec{\varepsilon}_{\|g}$ and $\vec{\varepsilon}_{\perp g}$ for DCR photons can be considered as the unit vectors of the spherical-coordinate system (situated in a plane perpendicular to the wave vector $\vec{\kappa}$). As a sequence, eq. (4) leads to the expression for the matrix element of DCR from axially channeled electrons:

$$(6)\qquad \left|M^{if}_{-g\tau}\right| = \frac{e}{2c}\frac{Q_{x\tau} + Q_{y\tau}}{\sqrt{1+W_\tau^2}}A_{\tau 0}.$$

Here, according to [3],

$$\begin{aligned}(7)\qquad W_\tau &= \Big(R - \left(|\chi_g|\, P_\tau\right)^2/R\Big)\Big/2\,|\chi_g|\,P_\tau, \quad \tau = \perp, \| \\ R &= \left(\theta_x - \mathrm{ctg}\theta_B\Omega_{if}/\omega_B\right)^2 + \theta_y^2 + \theta_{\mathrm{kin}}^2 - 2\Omega_{if}/\omega_B, \\ P_\tau &= \vec{\varepsilon}_{\tau 0}\vec{\varepsilon}_{\tau g}, \qquad \theta_{\mathrm{kin}}^2 = \gamma^{-2} + |\chi_0|\,,\end{aligned}$$

$\omega_B = c|\vec{g}|/(2\sin\theta_B)$ is the DCR photon frequency (*i.e.* after diffraction at the Bragg angle θ_B); $\chi_0 = \varepsilon_0 - 1$; χ_g are the Fourier components of dielectric susceptibility. In addition, the following notations are used:

$$\begin{aligned} &Q_{x\parallel} = P_\parallel x_{if}\left(\theta_x^2 - \Omega_{if}/\omega_B/\beta\right), \qquad Q_{y\parallel} = P_\perp y_{if}\theta_x\theta_y, \\ &Q_{x\perp} = P_\parallel x_{if}\theta_x\theta_y, \qquad Q_{y\perp} = P_\perp y_{if}\left(\theta_y^2 - \Omega_{if}/\omega_B/\beta\right), \end{aligned} \tag{8}$$

where $x_{if} = \langle\phi_f|x|\phi_i\rangle$ and $y_{if} = \langle\phi_f|y|\phi_i\rangle$ are the dipole transition matrix elements $i \to f$; $P_\parallel \equiv \vec{\varepsilon}_{\parallel g}\vec{\varepsilon}_{\parallel 0} \cong \cos 2\theta_B$, $P_\perp \equiv \vec{\varepsilon}_{\perp g}\vec{\varepsilon}_{\perp 0} = 1$. Equations (6)-(8) are obtained under the condition that the angular coordinates θ_x and θ_y are small enough (*i.e.* $\sin\theta_{x,y} \cong \theta_{x,y}$ and $\cos\theta_{x,y} \cong 1$).

3. – DCR polarization properties: general equations

The cross-section of photon emission at the Bragg angle is proportional to the square of the matrix element, $w_{if} \propto |M^{if}_{-g\tau}|^2$, therefore, for the degree of linear polarization we can write

$$\Pi = \frac{|M^{if}_{-g\perp}|^2 - |M^{if}_{-g\parallel}|^2}{|M^{if}_{-g\parallel}|^2 + |M^{if}_{-g\perp}|^2}\,. \tag{9}$$

The substitution of $M^{if}_{-g\tau}$ from eq. (6) into eq. (9) results in the formula for the degree of DCR linear polarization at axial channeling

$$(\Pi_{\mathrm{DCR}})_{\mathrm{axial}} = \frac{(Q_{y\perp} + Q_{x\perp})^2 W^2 - (Q_{y\parallel} + Q_{x\parallel})^2}{(Q_{y\perp} + Q_{x\perp})^2 W^2 + (Q_{y\parallel} + Q_{x\parallel})^2}, \qquad W = \sqrt{\frac{1 + W_\parallel^2}{1 + W_\perp^2}}\,. \tag{10}$$

If planar channeling takes place along the Y-direction, one can easily obtain the formula for DCR linear polarization from planar channeled electrons from eq. (10), making use of $(r_\perp)_x = x\vec{\varepsilon}_{\parallel 0} = 0$, $x_{if} = \langle\phi_f|x|\phi_i\rangle \equiv 0$, and hence $Q_{x\sigma} \equiv 0$. Thus, for the degree of DCR linear polarization from planar channeled electrons one obtains

$$(\Pi_{\mathrm{DCR}})_{\mathrm{planar}} = \frac{(Q_{y\perp})^2 W^2 - (Q_{y\parallel})^2}{(Q_{y\perp})^2 W^2 + (Q_{y\parallel})^2}\,. \tag{11}$$

The formula for the degree of linear polarization of PXR follows from eq. (11), if the transverse motion of channeled electron remains the same, *i.e.* $\hbar\Omega_{if} = 0$ $(i = f)$. Thus,

$$\Pi_{\mathrm{PXR}} = \frac{\theta_y^2 W^2 - \theta_x^2}{\theta_y^2 W^2 - \theta_x^2}, \qquad W \to W|_{\hbar\Omega_{if}=0}. \tag{12}$$

Further, if we consider that $|\chi_g|$ and $|\chi_0|$ are very small ($\approx 10^{-5}$), eq. (12) is reduced to the simple form

$$\Pi_{\mathrm{PXR}} \approx \frac{\theta_y^2 - \theta_x^2 P_\parallel^2}{\theta_y^2 + \theta_x^2 P_\parallel^2}\,. \tag{13}$$

For sufficiently small angles θ_x and θ_y (deviations from Bragg direction) and if $\theta_x = \theta_y$, formula (13) turns into the expression for the degree of PXR linear polarization used earlier to describe experimental data [10]

$$\Pi_{\mathrm{PXR}} \approx \frac{\sin^2 2\theta_B}{2 - \sin^2 2\theta_B} \,. \tag{14}$$

Note also that the smallness of $|\chi_g|$ and $|\chi_0|$ in eqs. (10)-(12) allows a simpler approximation for W to be written, *i.e.*

$$W = \sqrt{\frac{1 + W_{\parallel}^2}{1 + W_{\perp}^2}} \approx \frac{P_{\perp}}{P_{\parallel}} \approx \frac{1}{\cos 2\theta_B} \,. \tag{15}$$

This expression will be used in the next section.

4. – Linear polarization directions of DCR: Dependence on emission angle near the Bragg angle

In the same way as we defined the degree of linear polarization, see eq. (9), let us characterize the linear polarization direction of X-rays at the Bragg angle by the angle $\varphi = -\operatorname{Arctg}(|M^{if}_{-g\perp}|/|M^{if}_{-g\parallel}|)$ relative to the plane XZ. Then, using eq. (6) for the matrix elements of DCR at axial channeling, we get

$$(\varphi_{\mathrm{DCR}})_{\mathrm{axial}} = -\operatorname{Arctg}\left(\frac{Q_{y\perp} + Q_{x\perp}}{Q_{y\parallel} + Q_{x\parallel}} W\right), \qquad W = \sqrt{\frac{1 + W_{\parallel}^2}{1 + W_{\perp}^2}} \,. \tag{16}$$

Accordingly, let us denote the linear polarization direction of DCR at planar channeling by the angle

$$(\varphi_{\mathrm{DCR}})_{\mathrm{planar}} = -\operatorname{Arctg}\left(\frac{Q_{y\perp}}{Q_{y\parallel}} W\right). \tag{17}$$

Finally, the linear polarization direction of PXR (*i.e.*, when $\hbar\Omega_{if} = 0$) is characterized by the angle

$$\varphi_{\mathrm{PXR}} = -\operatorname{Arctg}\left(\frac{\theta_y}{\theta_x} W\right), \qquad W \to W|_{\hbar\Omega_{if}=0}. \tag{18}$$

The latter formula, in accordance with eq. (15), transforms into the well-known formula for the linear polarization direction of PXR [14, 16]

$$\operatorname{tg} \varphi_{\mathrm{PXR}} \approx -\frac{\theta_y}{\theta_x} \frac{1}{\cos 2\theta_B} \,. \tag{19}$$

Figures 2-5 show the angular distributions of DCR together with the maps of the DCR linear polarization directions calculated according to eq. (16). DCR is generated under different transitions $i \to f$ between the quantum states of the transverse motion

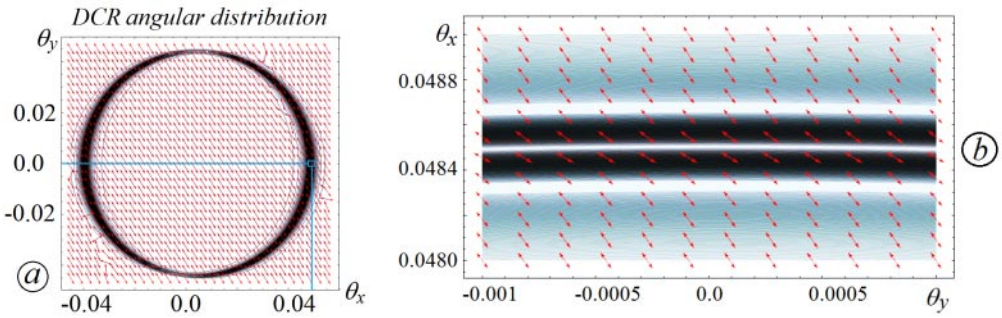

Fig. 2. – a) Schematics of the angular distribution of DCR in the vicinity of the Bragg angle $26°34'$. DCR is generated by $\gamma = 20$ electrons channelled along $\langle 100 \rangle$ Si, under the radiative transition $6 \to 5$. b) Map of the linear polarization directions of DCR calculated according eq. (16). The photon energy is 5.71 keV.

of electrons with $\gamma = 20$, channeled along $\langle 100 \rangle$ Si and $\langle 110 \rangle$ LiF axes. When electrons are channeled along the $\langle 100 \rangle$ Si direction, DCR is emitted in the vicinity of the Bragg angle $26°34'$, and in the case of $\langle 110 \rangle$ channeling in LiF, in the vicinity of the Bragg angle $18°26'$.

In figs. 2a-5a, on the ring of the angular distribution of DCR, we showed the points around which in figs. 2b-5b we show a map of the linear polarization directions of DCR.

Figures 2a and 2b show the map of the linear polarization directions of DCR generated by electrons channeled along $\langle 100 \rangle$ Si with $\gamma = 20$ and emitted in the vicinity of the Bragg angle $26°34'$. The map of linear polarization corresponds to a quantum transition between the electron transverse energy levels $6 \to 5$ (a ring of maximal DCR intensity). Figure 2a shows the angular distribution of DCR for this transition and formally presents a map of linear polarization directions of DCR for the entire area bounded by the ring of DCR. In fact, DCR does not equal zero only within the width of the DCR ring. Therefore, in fig. 2b we show the map of the linear polarization directions of DCR only for a small fragment of the whole DCR ring presented in fig. 2a. It should be mentioned that the linear polarization directions of DCR are changing remarkably inside the DCR ring.

Figure 3 presents similar results as in fig. 2, but for the quantum transition $4 \to 0$.

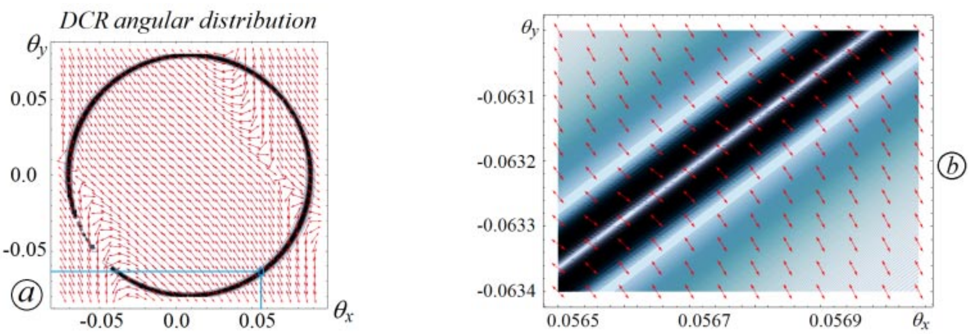

Fig. 3. – a) Angular distribution of DCR for transition $4 \to 0$ along $\langle 100 \rangle$ Si. b) Map of the linear polarization directions of DCR generated by electrons channelled along $\langle 100 \rangle$ Si with $\gamma = 20$ and emitted in the vicinity of the Bragg angle $26°34'$. The photon energy is 5.71 keV.

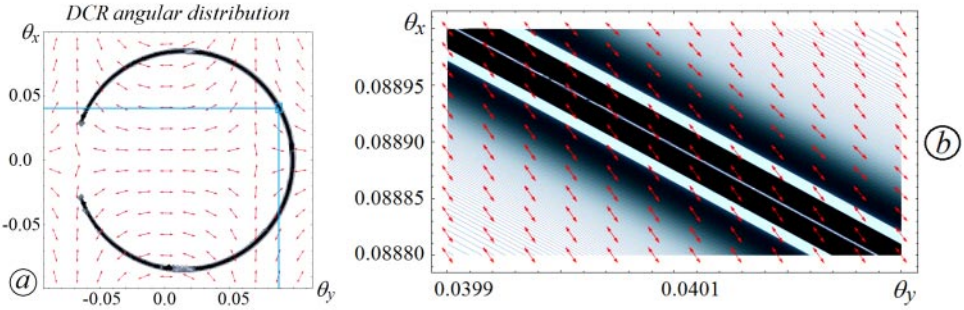

Fig. 4. – a) Angular distribution of DCR for transition $11 \to 2$ along $\langle 110 \rangle$ LiF. b) Map of the linear polarization directions of DCR generated by electrons channelled along $\langle 110 \rangle$ LiF with $\gamma = 20$ and emitted in the vicinity of the Bragg angle $18^\circ 26'$. The photon energy is 4.869 keV.

Figure 4 shows the results of calculations of DCR angular distributions and linear polarization generated by $\gamma = 20$ electrons channeled in $\langle 110 \rangle$ LiF under transition between quantum states of transverse motion $11 \to 2$. Contrary to figs. 2-3, here the change in direction of the linear polarization plane inside the DCR ring is negligible.

Finally, fig. 5 presents the results of calculations of DCR angular distributions and linear polarization generated by $\gamma = 20$ electrons planarly channeled in the (110) Si crystal under transition $2 \to 0$. As seen in fig. 4 (DCR from axially channeled electrons), the change in direction of the linear polarization plane inside the DCR ring is negligible.

5. – Conclusion

The results obtained suggest that the diffracted channeling radiation generated by both planar and axially channeled electrons is linearly polarized. The specific polarization properties of DCR can be formulated in comparison to PXR. Contrary to PXR, the map of the linear polarization directions of DCR:

i) Has two large regions of non-uniformity located far from the center of reflection, while a similar map of PXR has only one region near the center of reflection, around

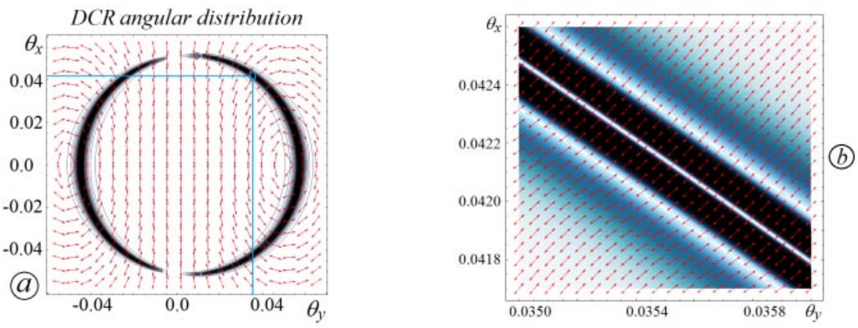

Fig. 5. – a) Angular distribution of DCR for transition $2 \to 0$ along (110) Si (planar channeling). b) Map of the linear polarization directions of DCR generated by electrons channeled along (110) Si with $\gamma = 20$ and emitted in the vicinity of the Bragg angle $22^\circ 30'$. The photon energy equals 5.169 keV.

the point with angular coordinates $\theta_x = \theta_y = 0$, and does not depend on a crystal type.

ii) Depends on the types of both a crystal and a quantum transition between transverse energy levels of channeled electron. For the transitions $i \to f$, corresponding to DCR rings of maximal intensities, at $\langle 100 \rangle$ axial channeling of $\gamma = 20$ electrons, the linear polarization directions change inside a DCR ring (see, figs. 2-3). This change vanishes in both the cases of LiF $\langle 100 \rangle$ axial and Si (110) planar channeling.

In view of a small angular width of the DCR peak intensity ($\approx$ 1–10 mrad), the experiments to observe either the effect of DCR or even the differences in the properties of the linear polarization directions of PXR and DCR might be rather complex. Recently, the intention to observe DCR was reported at the "Channeling 2010" Conference [18].

The authors believe that the performed studies of spectral-angular and polarization properties of DCR will help in some way to prepare and carry out these experiments.

* * *

The work is partially supported by the Russian Science and Innovations Federal Agency under contract No 02.740.11.0238 and by the Russian Fund for Basic Research, grant No 10–02–01386–a. We wish to thank Prof. H. Nitta for his interest and helpful discussions.

REFERENCES

[1] Ikeda T. *et al.*, *Nucl. Instrum. Methods B*, **115** (1996) 380.
[2] Matsuda Y. *et al.*, *Nucl. Instrum. Methods B*, **115** (1996) 396.
[3] Yabuki R. *et al.*, *Phys. Rev. B*, **63** (2001) 174112.
[4] Bogdanov O. V. *et al.*, *JETP Lett.*, **85** (2007) 555.
[5] Korotchenko K. B., *J. Surf. Invest. X-ray, Synchrotron Neutron Technol.*, **4** (2010) 599.
[6] Bogdanov O. V. *et al.*, *J. Surf. Invest. X-ray, Synchrotron Neutron Technol.*, **2** (2008) 290.
[7] Korotchenko K. B. *et al.*, *Nucl. Instrum. Methods B*, **266** (2008) 3753.
[8] Korotchenko K. B. *et al.*, *J. Phys.: Conf. Ser.*, **236** (2010) 012016.
[9] Korotchenko K. B. *et al.*, *J. Surf. Invest. X-ray, Synchrotron Neutron Technol.*, **4** (2010) 823.
[10] Adischev Yu. N. *et al.*, *Pis'ma Zh. Eksp. Teor. Fiz.*, **48(25)** (1988) 311.
[11] Shchagin A. V., *Phys. Lett. A*, **247** (1998) 27.
[12] Schmidt K. H. *et al.*, *Nucl. Instrum. Methods B*, **367** (1995) 215.
[13] They J. *et al.*, *Nucl. Instrum. Methods B*, **467-468** (2001) 1167.
[14] Morokhovskii V. V. *et al.*, *Phys. Rev. Lett.*, **79(22)** (1997) 4389.
[15] Baryshevsky V. G., Feranchuk I. D. and Ulyanenkov A. P., *Parametric X-ray Radiation in Crystals* (STMP 213, Springer) 2005, p. 213.
[16] Nitta H., *Radiat. Phys. Chem.*, **75** (2006) 1397.
[17] Ohtsuki Y. H., *Charged Beam Interaction with Solids* (Taylor & Francis Ltd., London & New York) 1983.
[18] Takabayashi Y. *et al.*, *Plan for Experimental Comparison of Diffracted Virtual and Real Photons Pattern*, presented at *Channeling 2010*, *Book of Abstracts*, 197.